Arthritis & Rheumatology
Vol. 0, No. 0, Month 2020, pp 1–11
DOI 10.1002/art.41180

American College of Rheumatology
Empowering Rheumatology Professionals

Negative Regulation of Osteoclast Commitment by Intracellular Protein Phosphatase Magnesium-Dependent 1A

Oh Chan Kwon,[1] Bongkun Choi,[2] Eun-Jin Lee,[2] Ji-Eun Park,[2] Eun-Ju Lee,[2] Eun-Young Kim,[2] Sang-Min Kim,[2] Min-Kyung Shin,[2] Tae-Hwan Kim,[3] Seokchan Hong,[2] Chang-Keun Lee,[2] Bin Yoo,[2] William H. Robinson,[4] Yong-Gil Kim,[2] and Eun-Ju Chang[2]

Objective. Increased protein phosphatase magnesium-dependent 1A (PPM1A) levels in patients with ankylosing spondylitis regulate osteoblast differentiation in bony ankylosis; however, the potential mechanisms that regulate osteoclast differentiation in relation to abnormal bone formation remain unclear. This study was undertaken to investigate the relationship of PPM1A to osteoclast differentiation by generating conditional gene-knockout (PPM1A$^{fl/fl}$;LysM-Cre) mice and evaluating their bone phenotype.

Methods. The bone phenotypes of LysM-Cre mice (n = 6) and PPM1A$^{fl/fl}$;LysM-Cre mice (n = 6) were assessed by micro–computed tomography. Osteoclast differentiation was induced by culturing bone marrow–derived macrophages in the presence of RANKL and macrophage colony-stimulating factor (M-CSF), and was evaluated by counting tartrate-resistant acid phosphatase–positive multinucleated cells. Levels of messenger RNA for *PPM*1A, *RANK*, and osteoclast-specific genes were examined by real-time quantitative polymerase chain reaction, and protein levels were determined by Western blotting. Surface RANK expression was analyzed by fluorescence flow cytometry.

Results. The PPM1A$^{fl/fl}$;LysM-Cre mice displayed reduced bone mass ($P < 0.001$) and increased osteoclast differentiation ($P < 0.001$) and osteoclast-specific gene expression ($P < 0.05$) compared with their LysM-Cre littermates. Mechanistically, reduced *PPM*1A function in osteoclast precursors in PPM1A$^{fl/fl}$;LysM-Cre mice induced osteoclast lineage commitment by up-regulating RANK expression ($P < 0.01$) via p38 MAPK activation in response to M-CSF. PPM1A expression in macrophages was decreased by Toll-like receptor 4 activation ($P < 0.05$). The Ankylosing Spondylitis Disease Activity Score was negatively correlated with the expression of PPM1A in peripheral blood mononuclear cells from patients with axial spondyloarthritis (SpA) ($\gamma = -0.7072$, $P < 0.0001$).

Conclusion. The loss of *PPM*1A function in osteoclast precursors driven by inflammatory signals contributes to osteoclast lineage commitment and differentiation by elevating RANK expression, reflecting a potential role of PPM1A in dynamic bone metabolism in axial SpA.

INTRODUCTION

Axial spondyloarthritis (SpA) is a chronic inflammatory disorder that primarily affects the axial skeleton, including the spine and sacroiliac joints (1). The characteristic features of axial SpA include new bone formation by the osteoproliferation of osteoblasts, which can eventually lead to bony ankylosis (1). Blocking the differentiation and activation of osteoblasts prevented radiographic progression in a mouse model of ankylosing spondylitis (AS) (2), which illustrates that osteoblasts represent an important component of bony ankylosis in AS. In addition, recent studies have focused on the divergent ability of osteoclast precursors to differentiate into

Supported by grants from the Basic Science and Engineering Research Program (2018-R1A2B2001867) and the National Research Foundation of Korea Medical Research Council (funded by the Korean government's Ministry of Science, ICT, and Future Planning) to Drs. Chang and Y.-G. Kim (2018-R1-5A2020732 and NRF-2019-R1F1A1059736, respectively).

[1]Oh Chan Kwon, MD: University of Ulsan College of Medicine, Asan Medical Center, and Yonsei University College of Medicine, Seoul, Republic of Korea; [2]Bongkun Choi, PhD, Eun-Jin Lee, PhD, Ji-Eun Park, MS, Eun-Ju Lee, PhD, Eun-Young Kim, PhD, Sang-Min Kim, MS, Min-Kyung Shin, MS, Seokchan Hong, MD, PhD, Chang-Keun Lee, MD, PhD, Bin Yoo, MD, PhD, Yong-Gil Kim, MD, PhD, Eun-Ju Chang, PhD: University of Ulsan College of Medicine and Asan Medical Center, Seoul, Republic of Korea; [3]Tae-Hwan Kim, MD, PhD: Hanyang University Hospital for Rheumatic Diseases, Seoul, Republic of Korea; [4]William H. Robinson, MD, PhD: Stanford University School of Medicine, Stanford, California.

Drs. Kwon, Choi, and Eun-Jin Lee contributed equally to this work.

No potential conflicts of interest relevant to this article were reported.

Address correspondence to Yong-Gil Kim, MD, PhD, or Eun-Ju Chang, PhD, University of Ulsan College of Medicine, Asan Medical Center, 88 Olympic-ro 43-gil, Songpa-gu, Seoul 05505, Korea. E-mail: bestmd2000@amc.seoul.kr or ejchang@amc.seoul.kr.

Submitted for publication January 30, 2019; accepted in revised form November 21, 2019.

osteoclasts during osteoclast commitment and accordingly influence bone-resorbing capacity in AS (3,4). Given that the bone remodeling process is coordinated by bone-resorbing osteoclasts and bone-forming osteoblasts (5), the pathophysiologic mechanisms underlying osteoproliferation in AS must be considered in terms of the coupling activities of osteoblasts and osteoclasts (2,3,6–8).

Bone-resorbing osteoclasts are derived from monocyte/macrophage precursors of the hematopoietic progenitor lineage. Proliferating macrophages serve as osteoclast precursors, which undergo further differentiation into osteoclasts (9). Two factors, namely macrophage colony-stimulating factor (M-CSF) and RANKL, are critical for osteoclast lineage commitment and differentiation (10–12). In the earlier stages of osteoclast differentiation, M-CSF binds to its receptor c-Fms on proliferating monocyte/macrophage precursors, thereby playing a key role in osteoclast lineage commitment prior to osteoclast differentiation (13) by activating transcription factors such as microphthalmia-associated transcription factor and PU.1 (14). Importantly, M-CSF can induce the expression of RANK, a receptor for RANKL, through MAPKs, including p38, JNK, and ERK (15,16). This induction of RANK typifies osteoclast lineage commitment. Following RANKL stimulation, the binding of TRAF6 to RANK results in the activation of MAPKs (17,18) and osteoclast-specific transcription factors, such as NFATc1 and NF-κB, to induce osteoclast-specific genes (10,19–21), leading to osteoclast differentiation (9,22). Therefore, in inflammatory conditions, the lineage commitment of macrophages is closely related to osteoclast activity, resulting in pathologic processes in bone remodeling in many diseases, such as osteoporosis, rheumatoid arthritis (RA), and AS (3,4,23).

Protein phosphatase magnesium-dependent 1A (PPM1A) is a member of the protein phosphatase 2C family of serine/threonine phosphatases (24). The expression of this protein is increased in cells or tissues under certain circumstances (25,26). We previously demonstrated that PPM1A levels are increased in the synovial tissue of patients with AS and that its up-regulation enhances osteoblast differentiation (25). Further, PPM1A expression is increased in macrophages during *Mycobacterium tuberculosis* infection, and this up-regulation plays a key role in the innate immune responses of macrophages (26). Considering that macrophages are the precursors of osteoclasts (9) and that PPM1A is known to inactivate MAPKs by dephosphorylating p38 and JNK (27), which are critical for RANK expression (17,18), PPM1A in macrophages might be a possible regulator of osteoclast differentiation.

In this study, we found that the down-regulation of the osteoclast precursor macrophage-specific *PPM1A* in mice resulted in apparently increased osteoclastogenesis, which occurs through the regulation of RANK expression. An inverse correlation between AS Disease Activity Score (ASDAS) and PPM1A expression level was also observed in peripheral blood mononuclear cells (PBMCs) obtained from patients with axial SpA. These discoveries establish PPM1A as a potential determinant of osteoclast lineage commitment from macrophages.

MATERIALS AND METHODS

Reagents and antibodies. RANKL and M-CSF were obtained from PeproTech. A tartrate-resistant acid phosphatase (TRAP) assay kit, lipopolysaccharide (LPS; from *Escherichia coli* O11:B4), PD98059, SB203580, SP60025, and β-actin antibodies were purchased from Sigma-Aldrich. Lipofectamine 2000 was purchased from Invitrogen. Phycoerythrin (PE)–conjugated anti-mouse CD265 (RANK), protease, and phosphatase inhibitor cocktails were purchased from ThermoFisher Scientific. Antibodies against PPM1A were purchased from Novus Biologicals. Antibodies against phospho-ERK, ERK, phospho-p38, p38, phospho-JNK, and JNK were purchased from Cell Signaling Technology. All antibodies used in this study were polyclonal antibodies raised from rabbits.

Mice and bone mineral density (BMD) measurements and histologic analysis. $PPM1A^{flox/flox}$ ($PPM1A^{fl/fl}$, MGI:4458753, $Ppm1a^{tm1a(EUCOMM)Hmgu}$) mice were purchased from MRC Harwell. To obtain mice with PPM1A-deficient macrophages, $PPM1A^{fl/fl}$ mice were bred with LysM-Cre mice (004781, B6.129P2-$Lyz2^{tm1(cre)Ifo}$/J; Jackson Laboratory). $PPM1A^{fl/fl}$;LysM-Cre mice were born at the expected Mendelian ratios, and they survived and reproduced as well as their wild-type (WT) littermates ($PPM1A^{fl/fl}$ or LysM-Cre mice). All mice in this study were from a pure C57BL/6 background. All animal procedures were approved by the Institutional Animal Care and Use Committee of the Asan Institute for Life Sciences (Seoul, Korea). Distal femurs dissected from the LysM-Cre mice and $PPM1A^{fl/fl}$;LysM-Cre mice (n = 6 per group) were fixed in 4% paraformaldehyde. Bone volume was measured by a micro–computed tomography analysis as previously described (28). Mouse hind limbs were collected for histologic analysis as previously described (28), and tissue sections were stained with hematoxylin and eosin or TRAP using an Acid Phosphatase Assay Kit (Sigma-Aldrich) according to the manufacturer's instructions. TRAP staining indicates the presence of mature osteoclasts. The osteoclast surface was assessed on TRAP-stained sections using ImageJ densitometry software, version 1.6 (National Institutes of Health).

Osteoclast differentiation. Bone marrow (BM) cells were isolated by flushing the marrow space in the femurs and tibiae collected from 6-week-old C57BL/6, LysM-Cre, $PPM1A^{fl/fl}$, and $PPM1A^{fl/fl}$;LysM-Cre mice. Mature osteoclasts were generated from BM-derived macrophages (BMMs) and were evaluated by TRAP staining as previously described (28,29). Briefly, isolated BMMs were cultured for 4 days with M-CSF (30 ng/ml) and RANKL (100 ng/ml) to induce differentiation into mature osteoclasts.

Reverse transcription–polymerase chain reaction (RT-PCR) and real-time quantitative PCR (qPCR) analysis. Total RNA was isolated from cells using TRIzol reagent (Life Technology), and 0.5–1 μg of RNA was reverse-transcribed using SuperScript II reverse transcriptase (Life Technologies). The resulting complementary DNA (cDNA) was amplified by PCR using the following primers: for mouse *PPM1A*, forward 5′-ATG-GTG-CAG-ATA-GAA-GCG-GG-3′ and reverse 5′-AGC-CAG-AGA-GCC-ATT-GAC-AC-3′; for mouse *DC-STAMP*, forward 5′-CCA-AGG-AGT-CGT-CCA-TGA-TT-3′ and reverse 5′-GGC-TGC-TTT-GAT-CGT-TTC-TC-3′; for mouse *OC-STAMP*, forward 5′-TTC-TCT-GGC-CTG-GAG-TTC-CT-3′ and reverse 5′-TGA-CAA-CTT-AGG-CTG-GGC-TG-3′; for mouse *CTSK*, forward 5′-AAT-ACC-TCC-CTC-TCG-ATC-CTA-CA-3′ and reverse 5′-GGT-TCT-TGA-CTG-GAG-TAA-CGT-A-3′; for mouse *TRAP*, forward 5′-TCC-TGG-CTC-AAA-AAG-CAG-TT-3′ and reverse 5′-ACA-TAG-CCC-ACA-CCG-TTC-TC-3′; for mouse *PU.1*, forward 5′-GAT-GGA-GAA-GCT-GAT-GGC-TTG-G-3′ and reverse 5′-TTC-TTC-ACC-TCG-CCT-GTC-TG-C-3′; for mouse *NFATc1*, forward 5′-GGG-TCA-GTG-TGA-CCG-AAG-AT-3′ and reverse 5′-GGA-AGT-CAG-AAG-TGG-GTG-GA-3′; for mouse *c-fms*, forward 5′-CCC-ACC-CTG-AAG-TCC-TGA-GT-3′ and reverse 5′-CTT-TGT-CCT-AGG-GAG-ACG-GC-3′; for mouse *RANK*, forward 5′-CAG-ATG-TCT-TTT-CGT-CCA-CAG-A-3′ and reverse 5′-AGA-CTG-GGC-AGG-TAA-GCC-T-3′; for mouse *GAPDH*, forward 5′-AGC-CAC-ATC-GCT-CAG-ACA-3′ and reverse 5′-GCC-CAA-TAC-GAC-CAA-ATC-C-3′; for human *PPM1A*, forward 5′-TGG-CGT-GTT-GAA-ATG-GAG-3′ and reverse 5′-AGC-GGA-TTA-CTT-GGT-TTG-TG-3′; for human *RANK*, forward 5′-AGA-TCG-CTC-CTC-CAT-GTA-CCA-3′ and reverse 5′-GCC-TTG-CCT-GTA-TCA-CAA-ACT-TT-3′; and for human *GAPDH*,

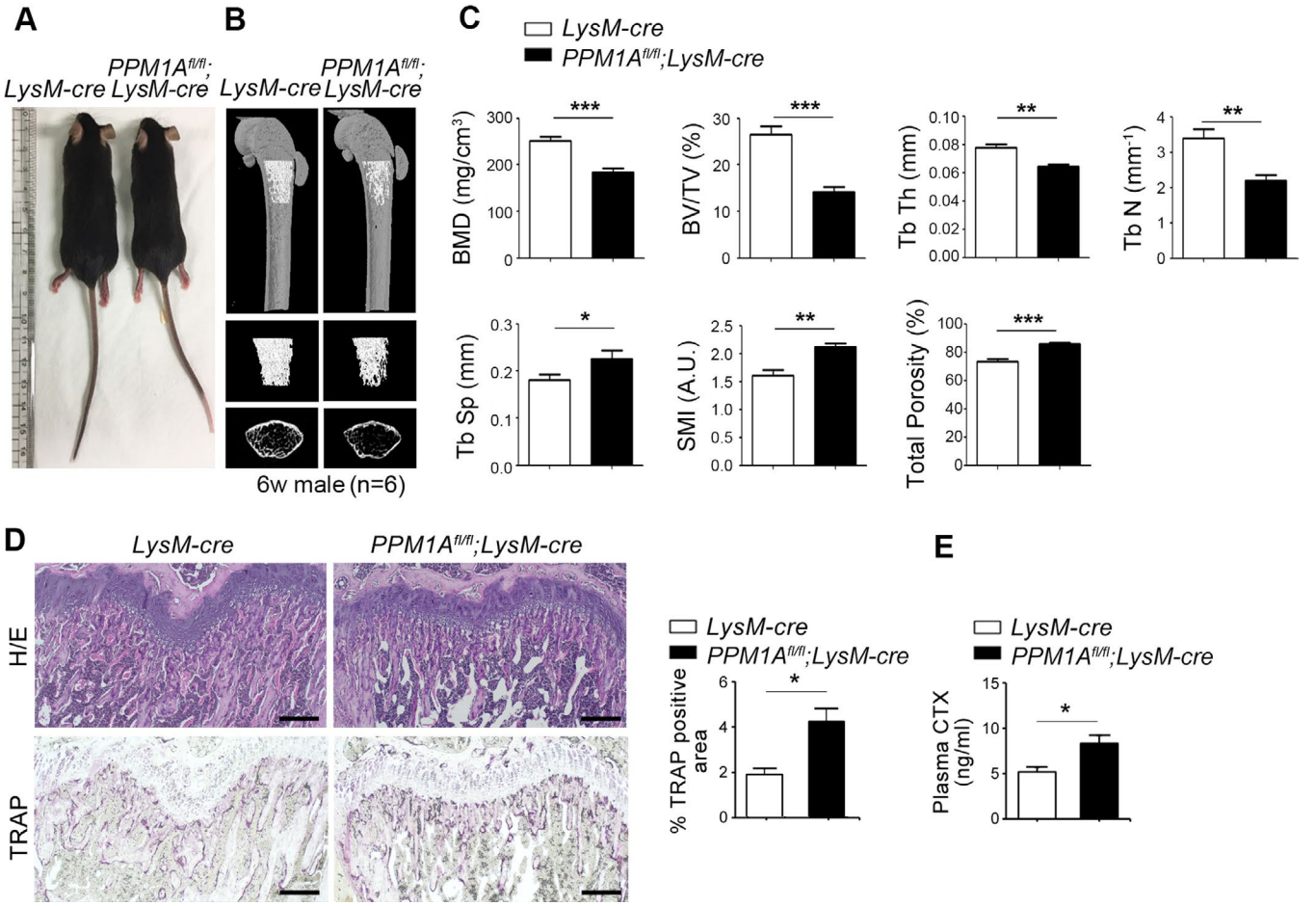

Figure 1. Bone phenotype in LysM-Cre mice and PPM1A$^{fl/fl}$;LysM-Cre mice. **A**, Comparison of the size of LysM-Cre mice and PPM1A$^{fl/fl}$;LysM-Cre mice. **B**, Micro–computed tomography images showing trabecular bone density in the femurs of 6-week-old LysM-Cre and PPM1A$^{fl/fl}$;LysM-Cre mice. **C**, Quantification of the features shown in **B**. BMD = bone mineral density; BV/TV = bone volume/total volume; TbTh = trabecular thickness; TbN = trabecular number; TbSp = trabecular separation; SMI = structure model index. **D**, Left, Hematoxylin and eosin (H&E) and tartrate-resistant acid phosphatase (TRAP) staining of hind limb sections from LysM-Cre and PPM1A$^{fl/fl}$;LysM-Cre mice. Mouse hind limbs were dissected, fixed, and decalcified, and the sections with the trabecular region were stained with H&E or TRAP (purple). Representative images from 3 independent experiments are shown. Bars = 200 μm. Right, Quantitation of the TRAP-positive surface area in sections from each mouse strain. **E**, Levels of C-terminal crosslinking telopeptide of type I collagen (CTX), a marker of bone turnover, in plasma from 6-week-old male LysM-Cre and PPM1Afl/fl;LysM-Cre mice, measured by enzyme-linked immunosorbent assay. Values in **C**, the right panel of **D**, and **E** are the mean ± SD of triplicate determinations (n = 6 mice per group). * = $P < 0.05$; ** = $P < 0.01$; *** = $P < 0.001$, by Mann-Whitney U test.

forward 5′-TGT-TGC-CAT-CAA-TGA-CCC-CTT-3′ and reverse 5′-CTC-CAC-GAC-GTA-CTC-AGC-G-3′. The PCR conditions and detailed procedure have been described previously (28). Real-time qPCR was performed using a Power SYBR Green 1-Step Kit and an ABI 7000 Real-Time PCR System (Applied Biosystems) according to the manufacturer's instructions.

Western blotting and fluorescence flow cytometry. Preparation of the cell lysates and sodium dodecyl sulfate–polyacrylamide gel electrophoresis gels and Western blot analyses were conducted according to a standard protocol (28). RANK expression on BMMs isolated from LysM-Cre and PPM1A$^{fl/fl}$;LysM-Cre mice was evaluated by incubating 5×10^5 cells with PE-conjugated anti-mouse RANK or an isotype control antibody in phosphate buffered saline (PBS) containing 2% fetal bovine serum at 4°C for 1 hour. The cells were washed twice with PBS. Flow cytometry was performed on a FACScan instrument according to the manufacturer's instructions (Becton Dickinson).

Reporter assay. The RANK promoter–luciferase reporter plasmid was transiently transfected into BMMs from WT and TLR-4–knockout mice using Lipofectamine 2000 according to the manufacturer's instructions. Two days after transfection, the cells were lysed using passive lysis buffer (Promega), and the luciferase activity in the extracts was measured using a Dual Luciferase assay system (Promega). Co-transfection with the *Renilla* vector allowed normalization of the assays for differences in transfection efficiency.

Human samples. PBMCs were collected from patients with axial SpA (n = 30) and age- and sex-matched healthy controls (n = 13) at the Asan Medical Center and Hanyang University Hospital. Clinical information was extracted from an electronic clinical database. All patients met the Assessment of SpondyloArthritis International Society classification criteria for axial SpA (30). Disease activity was determined using the ASDAS using the C-reactive protein level (ASDAS-CRP) (31). This study was approved by the institutional review boards of Asan Medical Center (IRB No. 2015-0274) and Hanyang University Hospital (IRB No. 2017-12-001).

Enzyme-linked immunosorbent assay (ELISA). The concentrations of C-terminal crosslinking telopeptide of type I collagen (CTX) (Mouse CTX-1 ELISA kit; Novus) in the plasma of LysM-Cre and PPM1Afl/fl;LysM-Cre mice were measured according to the manufacturer's protocols. All samples were examined in triplicate for each experiment.

Statistical analysis. Differences between the 2 groups were analyzed using the Mann-Whitney U test or Student's unpaired *t*-test, and the differences among 3 groups were analyzed by one-way analysis of variance. In the figures, bars are triplicate averages from single experiments, and a representative of 3 independent experiments is shown. The relationships between parameters were tested using Spearman's rank correlation coefficient. *P* values less than 0.05 were considered significant.

RESULTS

Macrophage-specific reduction in *PPM1A* expression in mice results in increased bone resorption due to enhanced osteoclast formation. To evaluate the effect of reduced *PPM1A* expression in macrophages (osteoclast precursors) on bone phenotype, we compared LysM-Cre and PPM1A$^{fl/fl}$;LysM-Cre mice at 6 weeks of age. Compared with LysM-Cre mice, the PPM1A$^{fl/fl}$;LysM-Cre mice were smaller (Figure 1A). CT revealed sparse trabecular bone density in PPM1A$^{fl/fl}$;LysM-Cre mice compared with LysM-Cre mice (Figure 1B). Accordingly, BMD, bone volume/total volume, trabecular thickness, and trabecular number were significantly lower and trabecular spacing and the structure model index were significantly greater in PPM1A$^{fl/fl}$;LysM-Cre mice, suggesting that bone resorption appears as a bone phenotype in PPM1A$^{fl/fl}$;LysM-Cre mice (Figure 1C). TRAP staining revealed enhanced osteoclast activity in PPM1A$^{fl/fl}$;LysM-Cre mice, as evidenced by the increased TRAP-positive staining (Figure 1D). Indeed, ELISA revealed that the level of CTX in the plasma of PPM1A$^{fl/fl}$;LysM-Cre mice was significantly higher than that in LysM-Cre mice, indicating that the reduced bone mass in PPM1A$^{fl/fl}$;LysM-Cre mice is caused by increased osteoclast activity (Figure 1E).

We next evaluated the expression status of osteoclast-specific genes (*TRAP*, *DC-STAMP*, *OC-STAMP*, and *CTSK*) (10,19–21,32) in macrophages from PPM1A$^{fl/fl}$;LysM-Cre and LysM-Cre mice. RT-PCR revealed lower *PPM1A* expression in macrophages from PPM1A$^{fl/fl}$;LysM-Cre mice than C57BL/6, LysM-Cre, and PPM1A$^{fl/fl}$ mice, as expected (Figure 2A). Consistent with this finding, PPM1A protein expression in macrophages was similarly decreased in PPM1A$^{fl/fl}$;LysM-Cre mice (Figure 2B). TRAP-positive mononuclear cells, which are osteoclast-specific lineage cells (33), were numerically increased in PPM1A$^{fl/fl}$;LysM-Cre mice (Figures 2C and D). Real-time qPCR illustrated that BMMs from PPM1A$^{fl/fl}$;LysM-Cre mice displayed higher *DC-STAMP*, *OC-STAMP*, *CTSK*, and *TRAP* expression than those from LysM-Cre mice (Figure 2E). These data suggest that reduced PPM1A expression in macrophages results in increased osteoclast differentiation due to the increased capacity for osteoclast formation in the early stages of osteoclast differentiation.

***PPM1A* down-regulation in macrophages leads to increased expression of RANK via p38 MAPK signaling.** To determine the mechanism by which PPM1A influences osteoclast commitment, we investigated the status of gene expression related to osteoclast lineage commitment (34) in M-CSF–cultured BMMs obtained from LysM-Cre and PPM1A$^{fl/fl}$;LysM-Cre mice. Real-time PCR revealed that *PU.1* messenger

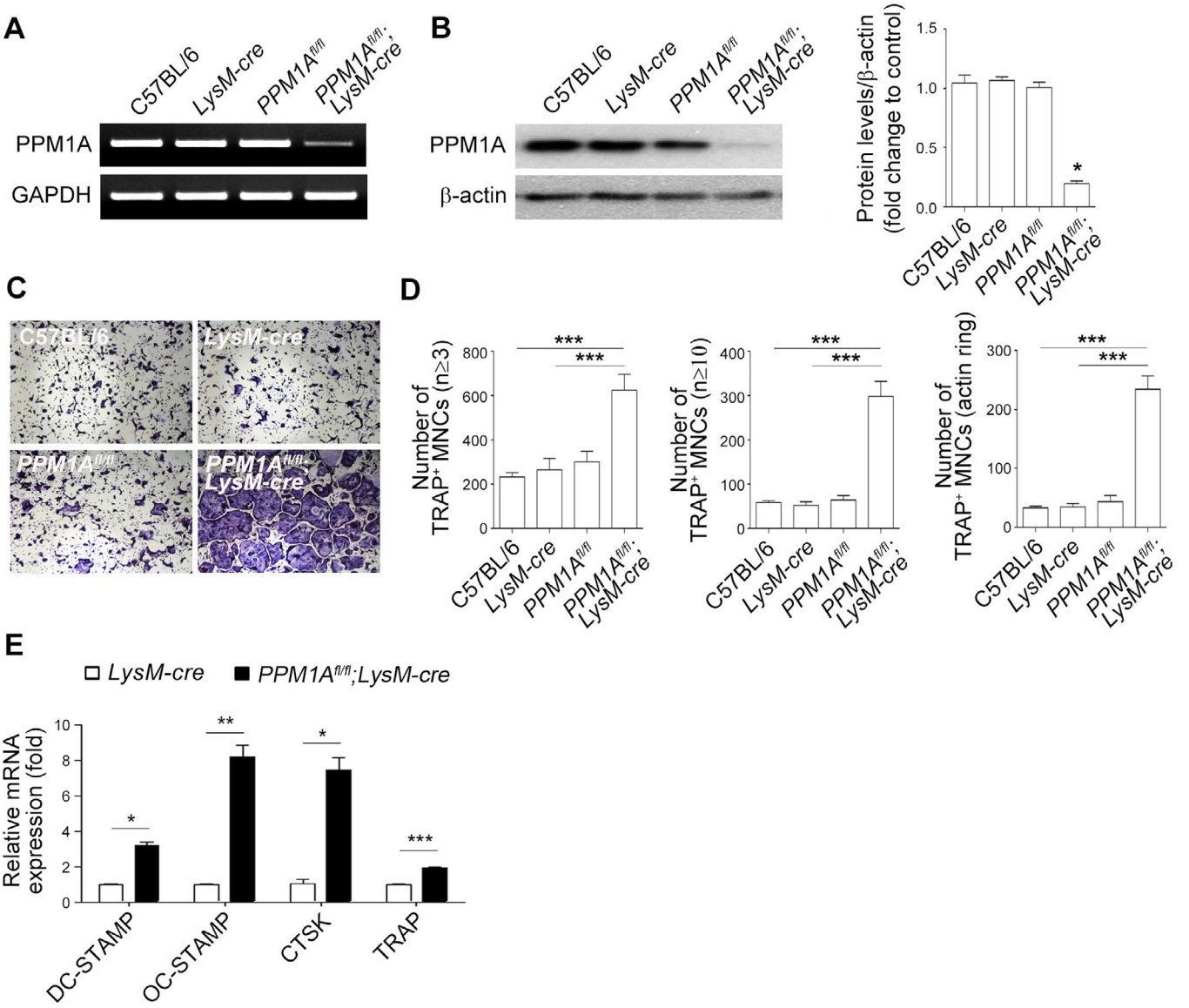

Figure 2. Association of decreased protein phosphatase magnesium-dependent 1A (PPM1A) expression in macrophages with increased expression of osteoclast-specific genes and osteoclast differentiation. **A** and **B**, *PPM1A* mRNA expression, determined by reverse transcription–polymerase chain reaction (PCR) (**A**), and PPM1A protein levels, determined by Western blotting (**B**), in macrophages from C57BL/6, LysM-Cre, PPM1A$^{fl/fl}$, and PPM1A$^{fl/fl}$;LysM-Cre mice. The right panel of **B** shows the densitometric quantification of PPM1A compared to β-actin. GAPDH was used as a loading control in **A**; β-actin was used as a loading control in **B**. **C**, Tartrate-resistant acid phosphatase (TRAP) staining for osteoclast formation. Macrophages from C57BL/6, LysM-Cre, PPM1A$^{fl/fl}$, and PPM1A$^{fl/fl}$;LysM-Cre mice were treated with macrophage colony-stimulating factor (30 ng/ml) and RANKL (100 ng/ml) for 4 days, fixed, and stained with TRAP. Original magnification × 200. **D**, Numbers of TRAP-positive multinucleated cells (MNCs) containing ≥3 nuclei, ≥10 nuclei, or an actin ring in **C**, counted under a light microscope. **E**, Relative expression of mRNA for the indicated osteoclast-specific genes in bone marrow–derived macrophages from LysM-Cre and PPM1A$^{fl/fl}$;LysM-Cre mice, determined by real-time quantitative PCR. The transcript levels were normalized to GAPDH. Values in the right panel of **B**, **D**, and **E** are the mean ± SD of triplicate determinations. * = $P < 0.05$; ** = $P < 0.01$; *** = $P < 0.001$, by Mann-Whitney U test. Color figure can be viewed in the online issue, which is available at http://onlinelibrary.wiley.com/doi/10.1002/art.41180/abstract.

RNA (mRNA) expression was increased in BMMs from PPM1A$^{fl/fl}$;LysM-Cre mice with no alteration in *c-fms* expression, suggesting that the osteoclast lineage commitment was enhanced by *PPM1A* down-regulation. Interestingly, *RANK* mRNA expression was increased in BMMs from PPM1A$^{fl/fl}$;LysM-Cre mice (Figure 3A). RANK protein expression was increased in macrophages from PPM1A$^{fl/fl}$;LysM-Cre mice compared with those from LysM-Cre mice (Figure 3B). Time-course Western blot analysis revealed no major changes in the activation of ERK or JNK upon M-CSF stimulation for 0–30 minutes compared with the LysM-Cre control (Figure 3C). Only p38 activation was increased in a time-dependent manner

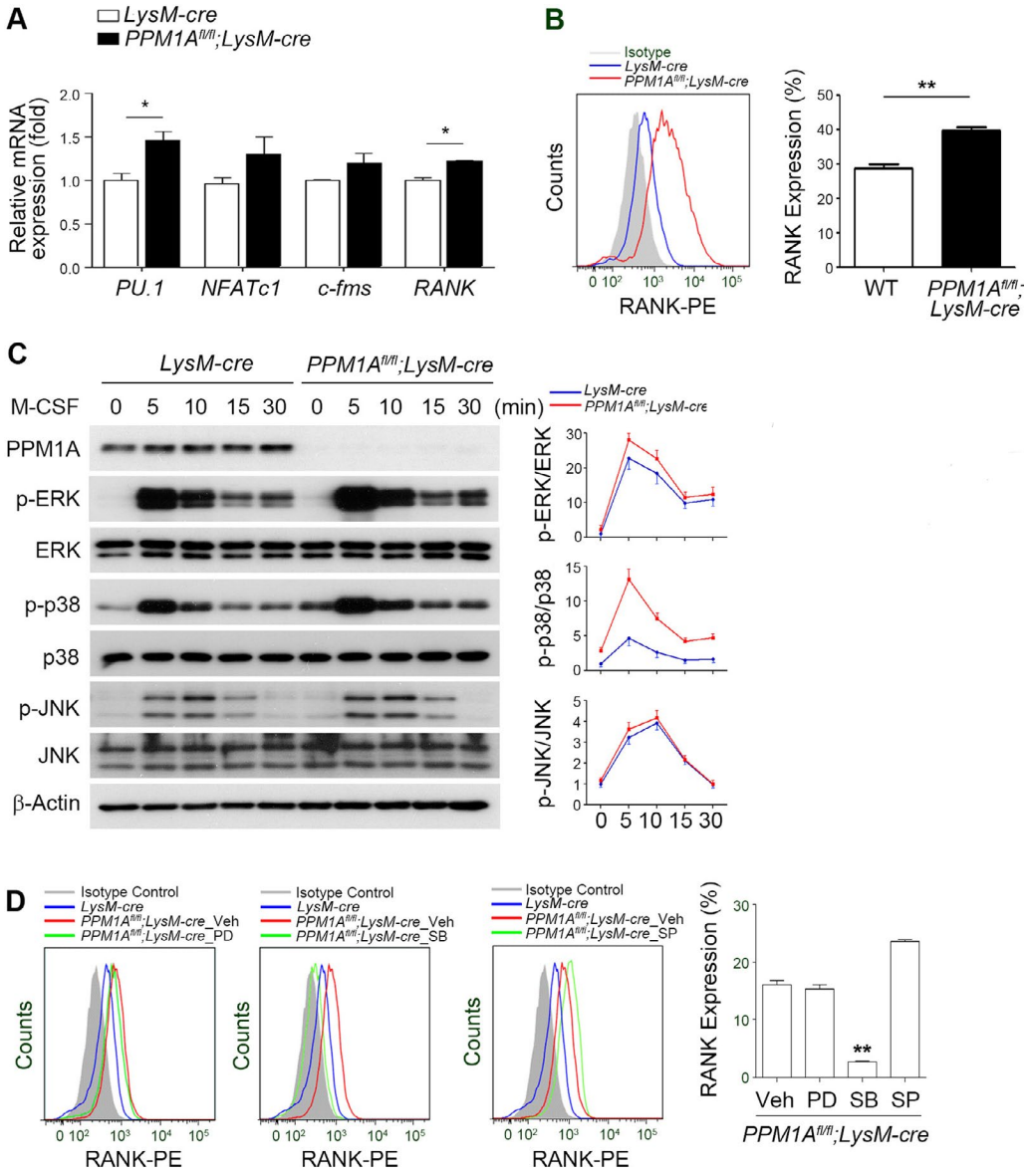

Figure 3. Increased expression of RANK in macrophages from PPM1A$^{fl/fl}$;LysM-Cre mice. **A**, Levels of expression of mRNA for genes involved in macrophage colony-stimulating factor (M-CSF) signaling and *RANK* in LysM-Cre (wild-type [WT]) and PPM1A$^{fl/fl}$;LysM-Cre mouse macrophages, determined by real-time quantitative polymerase chain reaction. **B**, Left, RANK expression in bone marrow–derived macrophages (BMMs) from LysM-Cre and PPM1A$^{fl/fl}$;LysM-Cre mice, analyzed by fluorescence flow cytometry. The shaded histogram indicates the isotype control. Right, Quantification of the percentage of phycoerythrin (PE)–conjugated RANK–positive cells. **C**, Left, Western blot analysis of M-CSF–induced activation of MAPKs (phospho-ERK, ERK, phospho-p38, p38, phospho-JNK, and JNK) in BMMs from LysM-Cre and PPM1A$^{fl/fl}$;LysM-Cre mice after stimulation with M-CSF for 0–30 minutes. Right, Quantification of the Western blot analysis results. **D**, Left, RANK expression in BMMs from LysM-Cre mice and PPM1A$^{fl/fl}$;LysM-Cre mice pretreated with DMSO (vehicle [veh]) and treated with an ERK inhibitor (PD98059 [PD]; 10 m*M*), a p38 inhibitor (SB203580 [SB]; 10 m*M*), or a JNK inhibitor (SP60025 [SP];10 m*M*) in the presence of M-CSF. Cells were analyzed for RANK expression by fluorescence flow cytometry. Right, Percentage of PE-conjugated RANK–positive cells. Values in **A** and the right panels of **B** and **D** are the mean ± SD of triplicate determinations. * = $P < 0.05$; ** = $P < 0.01$ by Mann-Whitney U test. Color figure can be viewed in the online issue, which is available at http://onlinelibrary.wiley.com/doi/10.1002/art.41180/abstract.

in PPM1A$^{fl/fl}$;LysM-Cre mouse macrophages compared with LysM-Cre mouse macrophages (Figure 3C).

To gain more direct evidence that PPM1A regulates *RANK* through p38 MAPK signaling, we treated BMMs with various MAPK inhibitors and analyzed RANK expression by flow cytometry. Consistent with the up-regulation of *RANK*, there was a significant difference in RANK levels in PPM1A$^{fl/fl}$;LysM-Cre mouse macrophages due to the activation of p38 MAPK (Figure 3D). These data indicate that PPM1A influences *RANK* expression through the p38 signaling pathway and that it may directly dephosphorylate p38 MAPK, as previously reported (35). Taken together, these findings show that PPM1A primarily regulates

RANK expression in mouse macrophages through the p38 signaling pathway.

LPS reduces PPM1A expression, resulting in increased RANK expression in macrophages. We next explored whether the inflammatory environment affects PPM1A expression. LPS, tumor necrosis factor, interleukin-1β (IL-1β), and IL-6 were used as the inflammatory stimuli. *PPM1A* mRNA and protein expression were diminished in macrophages from wild-type mice following LPS stimulation (Figures 4A and 4B). Because Toll-like receptor 4 (TLR-4) is the receptor for LPS (36–38), we then investigated whether PPM1A is downregulated in response to LPS exposure using TLR-4–knockout mice. Whereas LPS stimulation resulted in decreased *PPM1A* mRNA and protein expression in WT mouse macrophages, these effects were not observed in macrophages from TLR-4–knockout mice (Figures 4C and 4D). This regulatory axis affects RANK expression in macrophages, as evidenced by the finding that LPS stimulation increased *RANK* promoter activation (Figure 4E) and RANK expression (Figure 4F) in WT mouse macrophages but not in TLR-4–knockout mouse macrophages. Similarly, in human PBMCs, TLR-4 activation by LPS

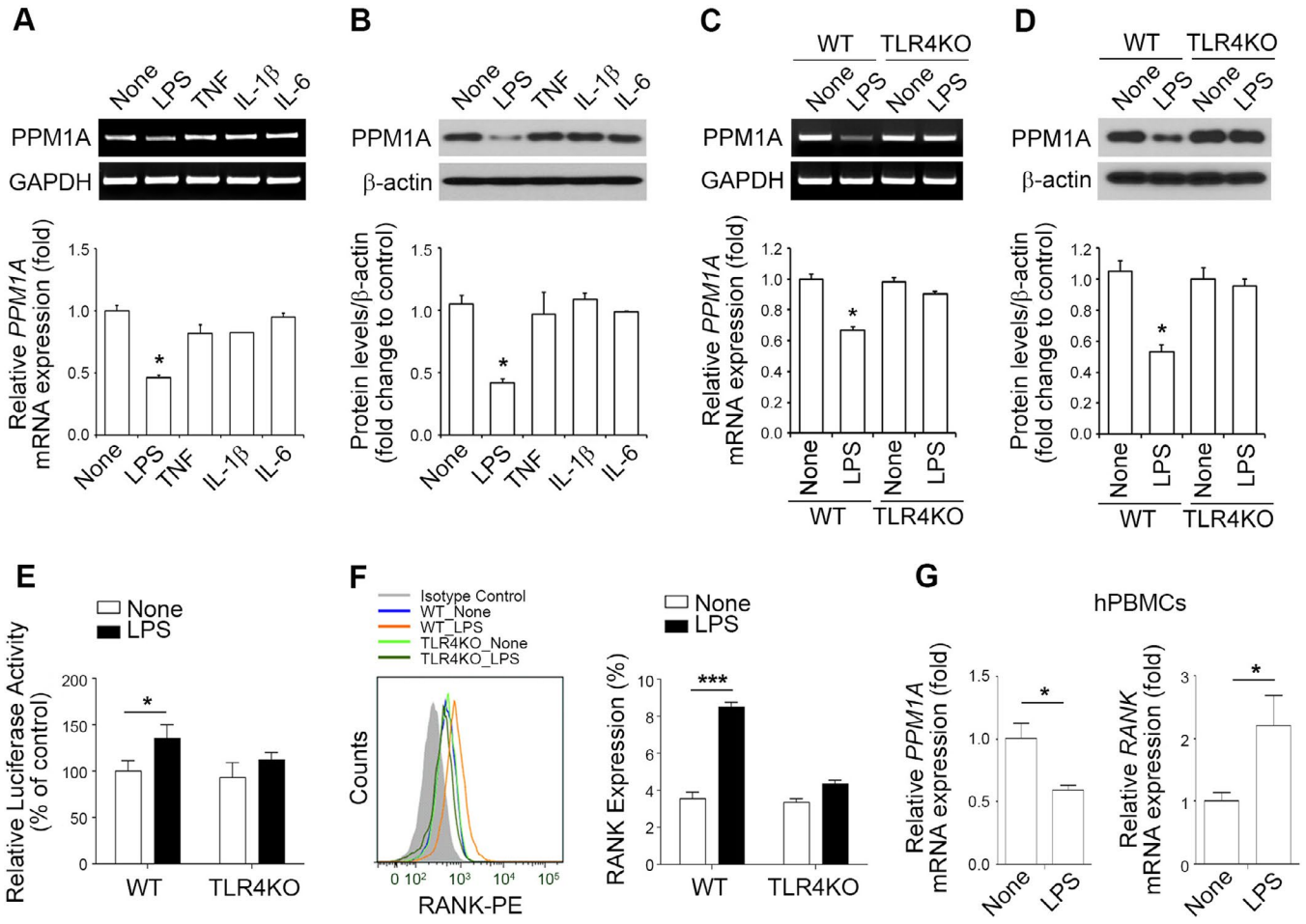

Figure 4. Reduced protein phosphatase magnesium-dependent 1A (PPM1A) expression and increased RANK expression in macrophages from wild-type mice stimulated with lipopolysaccharide (LPS). **A**, *PPM1A* mRNA expression in macrophages exposed to inflammatory stimuli including LPS, tumor necrosis factor (TNF), interleukin-1β (IL-1β), and IL-6, determined by reverse transcription–polymerase chain reaction (RT-PCR) (top) and quantitative RT-PCR (qRT-PCR) (bottom). **B**, PPM1A protein expression in macrophages treated with LPS, TNF, IL-1β, and IL-6, determined by Western blot analysis (top) and quantification of protein expression (bottom). **C**, *PPM1A* mRNA expression in macrophages from wild-type (WT) and TL-R4–knockout (TLR4KO) mice exposed to LPS, determined by RT-PCR (top) and qRT-PCR (bottom). **D**, PPM1A protein expression level in macrophages from WT and TLR-4–knockout mice exposed to LPS, determined by Western blotting (top), and quantification of protein expression (bottom). **E**, Relative luciferase activity in WT and TLR-4–knockout mice. Bone marrow–derived macrophages (BMMs) from WT and TLR-4–knockout mice were treated with LPS, and RANK promoter–luciferase reporter plasmids were transiently transfected into these cells. After 24 hours, the cells were harvested and subjected to the luciferase assay. Relative luciferase activity was normalized to control activity. **F**, Surface RANK protein level in WT and TLR-4–knockout mouse BMMs exposed to LPS, determined by flow cytometry. **G**, *PPM1A* and *RANK* mRNA expression levels in human peripheral blood mononuclear cells (hPBMCs) isolated from healthy controls and stimulated with LPS, determined by qRT-PCR. Values are the mean ± SD of triplicate determinations. * = $P < 0.05$; *** = $P < 0.001$, by Mann-Whitney U test. Color figure can be viewed in the online issue, which is available at http://onlinelibrary.wiley.com/doi/10.1002/art.41180/abstract.

stimulation was linked to decreased *PPM1A* mRNA expression, and this decrease was accompanied by an increase in *RANK* mRNA expression (Figure 4G).

PPM1A expression in PBMCs from patients with axial SpA. Because our results revealed a regulatory axis between PPM1A expression and the inflammatory condition,

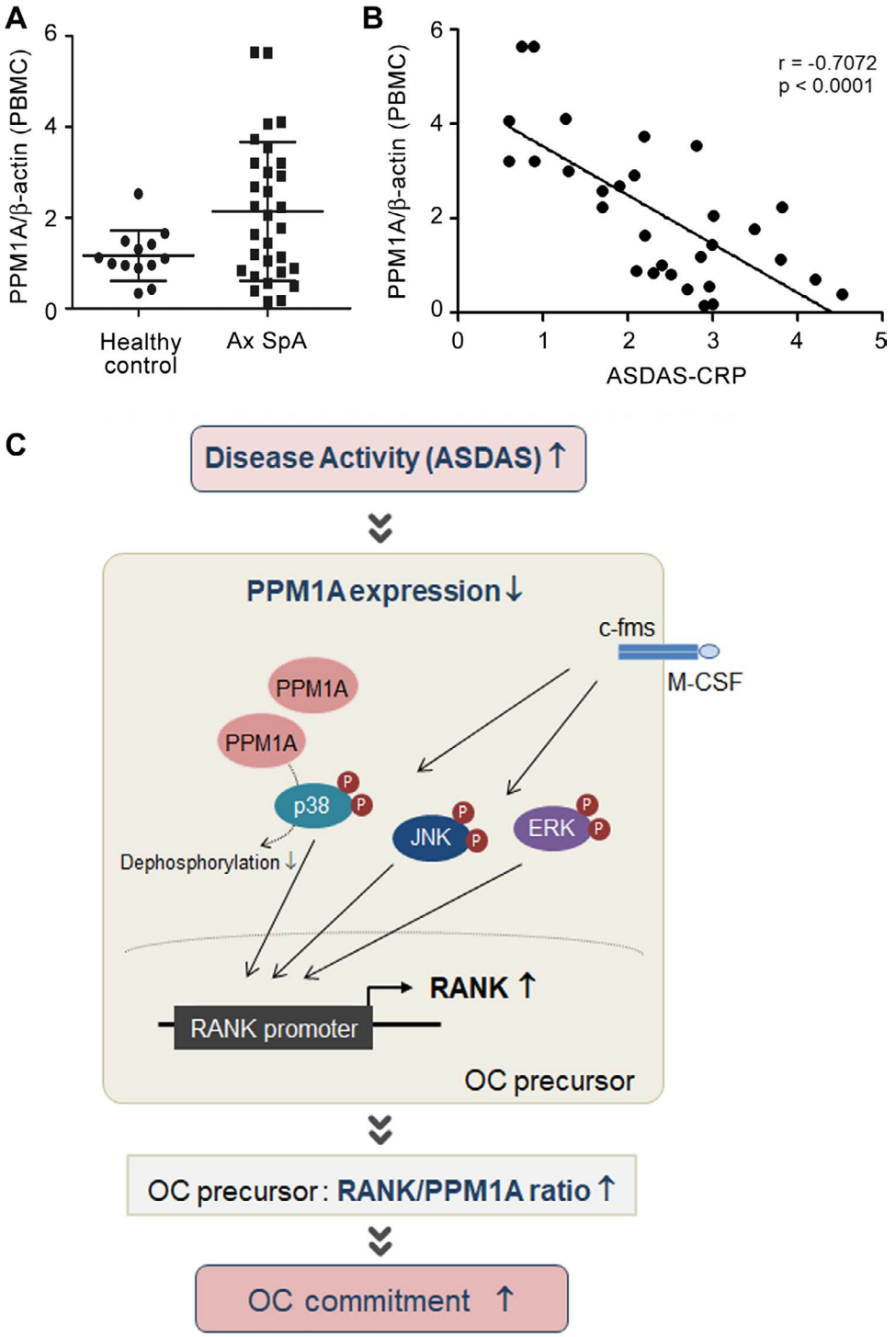

Figure 5. Lower expression levels of protein phosphatase magnesium-dependent 1A (PPM1A) in peripheral blood mononuclear cells (PBMCs) from patients with axial spondyloarthritis (Ax SpA) with higher disease activity. **A**, Protein levels of PPM1A in PBMCs from patients with axial SpA (n = 30) and age- and sex-matched healthy controls (n = 13), determined by immunoblot assay. Symbols represent individual subjects; horizontal lines and error bars show the mean ± SD. **B**, Correlation between PPM1A levels and Ankylosing Spondylitis Disease Activity Score using the C-reactive protein level (ASDAS-CRP) in patients with axial SpA (n = 30), determined by Spearman's correlation analysis. **C**, Suggested working model in axial SpA. M-CSF = macrophage colony-stimulating factor; OC = osteoclast. Color figure can be viewed in the online issue, which is available at http://onlinelibrary.wiley.com/doi/10.1002/art.41180/abstract.

Table 1. Characteristics of the 30 patients with axial spondyloarthritis*

Age, median (IQR) years	33.0 (28.5–42.0)
Male, no. (%)	28 (93.3)
Disease duration, median (IQR) months	19.2 (1.5–111.7)
HLA–B27 positive, no. (%)	29 (96.7)
Ankylosing spondylitis, no. (%)†	27 (90.0)
ASDAS-CRP, mean ± SD	2.35 ± 1.06

* IQR = interquartile range; ASDAS-CRP = Ankylosing Spondylitis Disease Activity Score using the C-reactive protein level.
† Patients who fulfilled the radiologic criterion of the 1984 modified New York criteria (sacroiliitis grade ≥2 bilaterally or grade 3–4 unilaterally).

it was important to determine whether there is a correlation between PPM1A expression and disease activity in axial SpA (7). We compared the PPM1A:β-actin ratio in PBMCs from patients with axial SpA (n = 30) and age- and sex-matched healthy controls (n = 13) and found that there was no significant difference (Figure 5A). Next, we evaluated whether the inflammatory burden, as measured by ASDAS-CRP, is correlated with PPM1A expression in PBMCs from patients with axial SpA (Figure 5B). Clinical variables for the patients with axial SpA are shown in Table 1. Of the 30 patients with axial SpA, 27 (90.0%) fulfilled the 1984 modified New York criteria for AS (39). In the correlation analysis, PPM1A expression in PBMCs and the ASDAS-CRP were negatively correlated ($r = -0.7072$, $P < 0.0001$), emphasizing that the inflammatory burden of axial SpA is associated with decreased PPM1A expression.

DISCUSSION

In this study, we demonstrated that the macrophage-specific down-regulation of *PPM1A* results in osteoclast commitment via increased RANK expression and enhanced RANK signaling. To our knowledge, this is the first study to identify the role of PPM1A in macrophages in osteoclast differentiation. We previously reported that PPM1A levels are increased in the synovial tissue of patients with AS and that PPM1A overexpression promotes osteoblast differentiation (25). The serum levels of PPM1A in patients with AS were also increased compared with those in patients with RA and in healthy controls (25). Although the serum PPM1A levels varied among patients with AS, the clinical significance of this variability has not been determined. In the present study, a greater range of PPM1A expression was also observed in PBMCs from patients with axial SpA. Those with higher expression of PPM1A in PBMCs may attenuate RANK expression more potently, resulting in the inhibition of osteoclast commitment and potential changes in the joint microstructure.

Osteoclasts are derived from hematopoietic stem cells (HSCs), and they are responsible for the resorption of endosteal bone surfaces and periosteal surfaces beneath the periosteum (10,40). RANK–RANKL interaction is the primary factor involved in osteoclast differentiation (9,22). RANKL binds to RANK expressed on the surface of osteoclast precursors and initiates downstream signaling (RANK signaling), which leads to the expression of osteoclast-specific genes and consequently the differentiation and activation of mature osteoclasts (9,22). Thus, the RANK level in osteoclast precursors can determine the capacity for osteoclast formation through osteoclast lineage commitment. We demonstrated that expression of mRNA for *RANK* and *PU.1* was increased in PPM1A$^{fl/fl}$;LysM-Cre mouse macrophages compared with LysM-Cre mouse macrophages. Considering that HSCs differentiate into osteoclast precursors in the presence of PU.1 under M-CSF signaling (33), we can conclude that macrophages from PPM1A$^{fl/fl}$;LysM-Cre mice display enforced osteoclast commitment due to M-CSF signaling. Notably, M-CSF, by binding to c-fms, autophosphorylates cytoplasmic tail tyrosine residues (41) and activates downstream events including p38 phosphorylation (42,43), resulting in increased RANK expression in early osteoclast precursors (44). Based on our results, we speculate that in circumstances in which PPM1A expression is decreased in macrophages, p38 activity increases, resulting in increased RANK expression and thereby enhanced osteoclast commitment.

The osteoclast-specific genes that are induced by RANK-mediated intracellular signaling include *CTSK*, *TRAP*, *CALCR*, *DC-STAMP*, *OC-STAMP*, and β3 integrin (10,19–21,32). In our study, the expression of mRNA for *CTSK*, *TRAP*, *DC-STAMP*, and *OC-STAMP* was increased in PPM1A$^{fl/fl}$;LysM-Cre mouse macrophages compared with LysM-Cre mouse macrophages, indicating that PPM1A down-regulates osteoclast-specific genes in these cells. Given that PPM1A inactivates MAPKs (27) and that MAPKs are important mediators of RANK-mediated intracellular signaling (17,18), PPM1A may attenuate further osteoclast differentiation by down-regulating RANK-mediated intracellular signaling stimulated by RANKL in osteoclast precursors. In particular, we found that LPS stimulation reduced PPM1A expression in macrophages, thus identifying inflammation as an important variable affecting *PPM1A* mRNA expression. Thus, in inflammatory conditions, osteoclast differentiation may be enhanced by increased RANK expression signaling attributable to PPM1A down-regulation in macrophages. However, the individual LPS-regulated inflammatory cytokines failed to suppress PPM1A. The reasons are not yet apparent, but we speculate that there could be additional mediators that stimulate TLR-4 signaling, such as pathogen-associated molecular patterns, rather than cytokine signaling that affects PP1MA.

In axial SpA, the severity of joint inflammation tends to fluctuate over time (45). Data in Figure 5A show that there was no significant difference in PPM1A expression in PBMCs from patients with axial SpA versus healthy controls. Although the explanation for this observation is unclear, the variability of axial SpA disease activity might have contributed to the greater range of PPM1A expression in PBMCs from patients with axial SpA. A strong negative correlation was observed between ASDAS-CRP and PPM1A expression in PMBCs, supporting the notion that the inflammatory burden is a possible regulator

of PPM1A expression. Interestingly, elevated serum levels of soluble RANKL and increased bone resorption as assessed by decreased BMD have also been reported in patients with AS (46). In that study, prominent elevation of soluble RANKL in patients with AS might have led to osteoclast commitment more actively in the presence of strong RANK expression in macrophages, thereby resulting in a resorptive bone phenotype. The notion that osteoclasts play a role in the pathogenesis of AS is supported by the clinical benefits resulting from treatment with pamidronate in active AS (47). Taken together, those findings and our results indicate that the PPM1A level may determine the resorptive bone phenotype in active axial SpA under an inflammatory burden by altering the capacity for osteoclast commitment in macrophages.

In conclusion, we demonstrated that PPM1A down-regulation in macrophages results in RANK up-regulation and RANK signaling enhancement, causing osteoclast commitment and further bone resorption. This finding suggests that PPM1A is both a potential enhancer of osteoblastogenesis (25) and a potential regulator of osteoclast commitment. Thus, in axial SpA with active inflammation, decreased PPM1A expression in PBMCs may enhance osteoclastogenesis via the up-regulation of RANK, thereby shifting the homeostasis of bone metabolism toward bone resorption (Figure 5B). These findings identify PPM1A as an important marker of bone metabolism in axial SpA and a potential therapeutic target for treating bony ankylosis.

AUTHOR CONTRIBUTIONS

All authors were involved in drafting the article or revising it critically for important intellectual content, and all authors approved the final version to be published. Dr. Y.-G. Kim had full access to all of the data in the study and takes responsibility for the integrity of the data and the accuracy of the data analysis.

Study conception and design. Robinson, Y.-G. Kim, Chang.

Acquisition of data. Kwon, Choi, Eun-Jin Lee, T.-H. Kim, Hong, C.-K. Lee, Yoo, Y.-G. Kim, Chang.

Analysis and interpretation of data. Kwon, Choi, Eun-Jin Lee, Park, Eun-Ju Lee, E.-Y. Kim, S.-M. Kim, Shin, Y.-G. Kim, Chang.

REFERENCES

1. Taurog JD, Chhabra A, Colbert RA. Ankylosing spondylitis and axial spondyloarthritis [review]. N Engl J Med 2016;374:2563–74.
2. Lories RJ, Derese I, Luyten FP. Modulation of bone morphogenetic protein signaling inhibits the onset and progression of ankylosing enthesitis. J Clin Invest 2005;115:1571–9.
3. Perpétuo IP, Caetano-Lopes J, Vieira-Sousa E, Campanilho-Marques R, Ponte C, Canhão H, et al. Ankylosing spondylitis patients have impaired osteoclast gene expression in circulating osteoclast precursors. Front Med (Lausanne) 2017;4:5.
4. Perpétuo IP, Raposeiro R, Caetano-Lopes J, Vieira-Sousa E, Campanilho-Marques R, Ponte C, et al. Effect of tumor necrosis factor inhibitor therapy on osteoclasts precursors in ankylosing spondylitis. PLoS One 2015;10:e0144655.
5. Khosla S. Pathogenesis of age-related bone loss in humans. J Gerontol A Biol Sci Med Sci 2013;68:1226–35.
6. Lories R. The balance of tissue repair and remodeling in chronic arthritis [review]. Nat Rev Rheumatol 2011;7:700–7.
7. Zhang X, Aubin JE, Inman RD. Molecular and cellular biology of new bone formation: insights into the ankylosis of ankylosing spondylitis. Curr Opin Rheumatol 2003;15:387–93.
8. Tam LS, Gu J, Yu D. Pathogenesis of ankylosing spondylitis [review]. Nat Rev Rheumatol 2010;6:399–405.
9. Boyle WJ, Simonet WS, Lacey DL. Osteoclast differentiation and activation [review]. Nature 2003;423:337–42.
10. Arai F, Miyamoto T, Ohneda O, Inada T, Sudo T, Brasel K, et al. Commitment and differentiation of osteoclast precursor cells by the sequential expression of c-Fms and receptor activator of nuclear factor κB (RANK) receptors. J Exp Med 1999;190:1741–54.
11. Cappellen D, Luong-Nguyen NH, Bongiovanni S, Grenet O, Wanke C, Šuša M. Transcriptional program of mouse osteoclast differentiation governed by the macrophage colony-stimulating factor and the ligand for the receptor activator of NFκB. J Biol Chem 2002;277:21971–82.
12. Dougall WC, Glaccum M, Charrier K, Rohrbach K, Brasel K, De Smedt T, et al. RANK is essential for osteoclast and lymph node development. Genes Dev 1999;13:2412–24.
13. Tanaka S, Takahashi N, Udagawa N, Tamura T, Akatsu T, Stanley ER, et al. Macrophage colony-stimulating factor is indispensable for both proliferation and differentiation of osteoclast progenitors. J Clin Invest 1993;91:257–63.
14. Nakanishi A, Hie M, Iitsuka N, Tsukamoto I. A crucial role for reactive oxygen species in macrophage colony-stimulating factor-induced RANK expression in osteoclastic differentiation. Int J Mol Med 2013;31:874–80.
15. Lee K, Chung YH, Ahn H, Kim H, Rho J, Jeong D. Selective regulation of MAPK signaling mediates RANKL-dependent osteoclast differentiation. Int J Biol Sci 2016;12:235–45.
16. Sobacchi C, Frattini A, Guerrini MM, Abinun M, Pangrazio A, Susani L, et al. Osteoclast-poor human osteopetrosis due to mutations in the gene encoding RANKL. Nat Genet 2007;39:960–2.
17. Li X, Udagawa N, Itoh K, Suda K, Murase Y, Nishihara T, et al. P38 MAPK-mediated signals are required for inducing osteoclast differentiation but not for osteoclast function. Endocrinology 2002;143:3105–13.
18. Matsumoto M, Sudo T, Saito T, Osada H, Tsujimoto M. Involvement of p38 mitogen-activated protein kinase signaling pathway in osteoclastogenesis mediated by receptor activator of NF-κ B ligand (RANKL). J Biol Chem 2000;275:31155–61.
19. Wada T, Nakashima T, Hiroshi N, Penninger JM. RANKL-RANK signaling in osteoclastogenesis and bone disease. Trends Mol Med 2006;12:17–25.
20. Boyce BF. Advances in osteoclast biology reveal potential new drug targets and new roles for osteoclasts [review]. J Bone Miner Res 2013;28:711–22.
21. Edwards JR, Mundy GR. Advances in osteoclast biology: old findings and new insights from mouse models [review]. Nat Rev Rheumatol 2011;7:235–43.
22. Suda T, Takahashi N, Udagawa N, Jimi E, Gillespie MT, Martin TJ. Modulation of osteoclast differentiation and function by the new members of the tumor necrosis factor receptor and ligand families [review]. Endocr Rev 1999;20:345–57.
23. Takayanagi H. Osteoimmunology: shared mechanisms and crosstalk between the immune and bone systems [review]. Nat Rev Immunol 2007;7:292–304.
24. Zolnierowicz S. Type 2A protein phosphatase, the complex regulator of numerous signaling pathways. Biochem Pharmacol 2000;60:1225–35.
25. Kim YG, Sohn DH, Zhao X, Sokolove J, Lindstrom TM, Yoo B, et al. Role of protein phosphatase magnesium-dependent 1A and

anti–protein phosphatase magnesium-dependent 1A autoantibodies in ankylosing spondylitis. Arthritis Rheumatol 2014;66:2793–803.

26. Sun J, Schaaf K, Duverger A, Wolschendorf F, Speer A, Wagner F, et al. Protein phosphatase, Mg2+/Mn2+-dependent 1A controls the innate antiviral and antibacterial response of macrophages during HIV-1 and Mycobacterium tuberculosis infection. Oncotarget 2016;7:15394–409.
27. Takekawa M, Maeda T, Saito H. Protein phosphatase 2Cα inhibits the human stress-responsive p38 and JNK MAPK pathways. EMBO J 1998;17:4744–52.
28. Lee EJ, Kim SM, Choi B, Kim EY, Chung YH, Lee EJ, et al. Interleukin-32 γ stimulates bone formation by increasing miR-29a in osteoblastic cells and prevents the development of osteoporosis. Sci Rep 2017;7:40240.
29. Lee EJ, Song DH, Kim YJ, Choi B, Chung YH, Kim SM, et al. PTX3 stimulates osteoclastogenesis by increasing osteoblast RANKL production. J Cell Physiol 2014;229:1744–52.
30. Rudwaleit M, van der Heijde D, Landewé R, Listing J, Akkoc N, Brandt J, et al. The development of Assessment of SpondyloArthritis international Society classification criteria for axial spondyloarthritis. Part II. Validation and final selection. Ann Rheum Dis 2009;68:777–83.
31. Lukas C, Landewé R, Sieper J, Dougados M, Davis J, Braun J, et al. Development of an ASAS-endorsed disease activity score (ASDAS) in patients with ankylosing spondylitis. Ann Rheum Dis 2009;68:18–24.
32. Lacey DL, Timms E, Tan HL, Kelley MJ, Dunstan CR, Burgess T, et al. Osteoprotegerin ligand is a cytokine that regulates osteoclast differentiation and activation. Cell 1998;93:165–76.
33. Amarasekara DS, Yun H, Kim S, Lee N, Kim H, Rho J. Regulation of osteoclast differentiation by cytokine networks. Immune Netw 2018;18:e8.
34. Boyce BF. Advances in the regulation of osteoclasts and osteoclast functions. J Dent Res 2013;92:860–7.
35. Dvashi Z, Sar Shalom H, Shohat M, Ben-Meir D, Ferber S, Satchi-Fainaro R, et al. Protein phosphatase magnesium dependent 1A governs the wound healing-inflammation-angiogenesis cross talk on injury. Am J Pathol 2014;184:2936–50.
36. Poltorak A, He X, Smirnova I, Liu MY, Van Huffel C, Du X, et al. Defective LPS signaling in C3H/HeJ and C57BL/10ScCr mice: mutations in Tlr4 gene. Science 1998;282:2085–8.
37. Qureshi ST, Larivière L, Leveque G, Clermont S, Moore KJ, Gros P, et al. Endotoxin-tolerant mice have mutations in Toll-like receptor 4 (Tlr4). J Exp Med 1999;189:615–25.
38. Hoshino K, Takeuchi O, Kawai T, Sanjo H, Ogawa T, Takeda Y, et al. Cutting edge: Toll-like receptor 4 (TLR4)-deficient mice are hyporesponsive to lipopolysaccharide: evidence for TLR4 as the Lps gene product. J Immunol 1999;162:3749–52.
39. Van der Linden S, Valkenburg HA, Cats A. Evaluation of diagnostic criteria for ankylosing spondylitis: a proposal for modification of the New York criteria. Arthritis Rheum 1984;27:361–8.
40. Zaidi M. Skeletal remodeling in health and disease. Nat Med 2007; 13:791–801.
41. Feng X, Takeshita S, Namba N, Wei S, Teitelbaum SL, Ross FP. Tyrosines 559 and 807 in the cytoplasmic tail of the macrophage colony-stimulating factor receptor play distinct roles in osteoclast differentiation and function. Endocrinology 2002;143:4868–74.
42. Wang Y, Piper MG, Marsh CB. The role of Src family kinases in mediating M-CSF receptor signaling and monocytic cell survival. Adv Biosci Biotechnol 2012;3:592–602.
43. Wang Y, Zeigler MM, Lam GK, Hunter MG, Eubank TD, Khramtsov VV, et al. The role of the NADPH oxidase complex, p38 MAPK, and Akt in regulating human monocyte/macrophage survival. Am J Respir Cell Mol Biol 2007;36:68–77.
44. Soysa NS, Alles N, Aoki K, Ohya K. Osteoclast formation and differentiation: an overview. J Med Dent Sci 2012;59:65–74.
45. Stone MA, Pomeroy E, Keat A, Sengupta R, Hickey S, Dieppe P, et al. Assessment of the impact of flares in ankylosing spondylitis disease activity using the Flare Illustration. Rheumatology (Oxford) 2008;47:1213–8.
46. Kim HR, Lee SH, Kim HY. Elevated serum levels of soluble receptor activator of nuclear factors-κB ligand (sRANKL) and reduced bone mineral density in patients with ankylosing spondylitis (AS). Rheumatology (Oxford) 2006;45:1197–200.
47. Maksymowych WP, Jhangri GS, Fitzgerald AA, LeClercq S, Chiu P, Yan A, et al. A six-month randomized, controlled, double-blind, dose-response comparison of intravenous pamidronate (60 mg versus 10 mg) in the treatment of nonsteroidal antiinflammatory drug–refractory ankylosing spondylitis. Arthritis Rheum 2002;46:766–73.